Hindawi
Geofluids
Volume 2021, Article ID 8871535, 12 pages
https://doi.org/10.1155/2021/8871535

Research Article

Effect of Seepage Force on the Wellbore Breakdown of a Vertical Wellbore

Desheng Zhou[1,2] **Haiyang Wang**[1] **Yafei Liu**[1,2] **Shun Liu**[2] **Xianlin Ma**[1] **Wenbin Cai**[1] **and Hai Huang**[1,2]

[1]*School of Petroleum Engineering, Xi'an Shiyou University, Xi'an 710065, China*
[2]*Engineering Research Center of Development and Management for Low to Extra-Low Permeability Oil & Gas Reservoirs in West China, Ministry of Education, Xi'an Shiyou University, Xi'an, 710065 Shaanxi, China*

Correspondence should be addressed to Desheng Zhou; deshengzhou@126.com

Received 16 May 2020; Revised 20 September 2020; Accepted 20 March 2021; Published 8 April 2021

Academic Editor: Mauro Giudici

As a fluid flows through a porous media, a drag force, called seepage force in the paper, will be formed on the matrix of the media in the fluid flowing direction. However, the seepage force is normally ignored in the analysis of wellbore fracturing during hydraulic fracturing operation. In this paper, an analytical model for seepage force around a vertical wellbore is presented based on linear elasticity theory, and the effect of the seepage force on wellbore breakdown has been analyzed. Also studied are the effects of the two horizontal principal stresses and the reservoir permeability on the action of seepage force. The paper proves that seepage force lowers formation breakdown pressure of a vertical wellbores; the deeper a formation is, the greater action of the seepage force; seepage force contributes more to breakdown formation with small difference of the two horizontal stresses such as unconventional reservoirs; seepage force increases as rock permeability decreases, and it should not be ignored in hydraulic fracturing analysis, especially for low-permeability formation.

1. Introduction

The evaluation of the stress fields around wellbores in porous media attracts plenty of interests due to its relevance in oil and gas production, with special emphasis on hydraulic fracturing. The distributions of the stress and pore pressure fields in wellbore rock are essential to studying the initiation of hydraulic fractures.

Haimson and Fairhurst [1–4] systematically studied the stress field around a wellbore during the initiation of fractures and proposed that when fluid was injected into a wellbore, three stress fields acted together to induce the breakdown of permeable reservoirs. These three stress fields include in situ stress, wellbore pressure, and poroelastic stress caused by pore pressure variations in wellbore rock after wellbore fluid flows into a reservoir.

Hubbert and Willis [5] and Medlin and Masse [6] investigated the mechanics of hydraulic fracture initiation by comparing laboratory experiments with theoretical predictions based on poroelasticity. In the recent 20 years, quite a few scholars [7–11] have analyzed the influencing factors of formation breakdown pressure based on Haimson's theory combined with experimental results.

Based on the model of Hubbert and Hamison, Ito [12, 13] proposed a newly constructed fracture criterion that can explain the effects of wellbore diameter and pressurization rate on the breakdown pressure. Jin et al. [14] presented a weight function method to predict the breakdown pressure of two general symmetrical radial fractures emanating from a wellbore. Fatahi et al. [15] presented a simulation model based on a distinct element method to study the breakdown pressure during hydraulic fracturing tests. Xiao et al. [16] proposed a fracture initiation model for carbon dioxide fracturing under various bottom hole pressure and temperature conditions.

However, flowing into reservoir rock of wellbore fluid not only increases in situ pore pressure and thus creates poroelastic stress but also results in a pore pressure gradient along the fluid flowing direction in wellbore rock. Under the action of

fluid dragging, the flowing fluid exerts a force, called seepage force, on rock skeleton affecting stress fields around the wellbore. Mourgues et al. [17], Cobbold et al. [18], and Zanella and Cobbold [19] verified the existence of the seepage force during fluid flowing in a porous media based on sandbox experiments and evaluated the influence of seepage force on media structure. Rozhko et al. [20, 21] investigated the influence of seepage force on the failure of a porous elastic media and calculated the stress field created by the seepage force. Zhou et al. [22] analyzed the behavior of stabilizing piles for landslides in the Three Gorges Reservoir under the effect of seepage force. Zou et al. [23] derived theoretical solutions for a circular opening in an elastic-brittle-plastic rock mass incorporating the out-of-plane stress and seepage force. AlKhafaji et al. [24] studied the bearing capacity problem of shallow rigid foundations on rock matrix subjected to horizontal seepage force.

Although the seepage force has been proved and discussed in soil engineering, and applied in dam stability analysis for decades, it has been ignored in oil and gas production. Few literatures in hydraulic fracturing analysis discuss the effect of the seepage force on hydraulic fracturing process.

In this work, seepage force will be introduced into the analysis of a vertical well during hydraulic fracturing operation. A model analyzing the stress field around the wellbore by seepage force will be presented. To study the effect of seepage force, traditional stress field analyses around the wellbore during hydraulic fracturing process will be discussed firstly. Seepage force contribution to the wellbore breakdown will be compared by the results from cases with and without considering the seepage force. Also explored are the effects of formation confining pressure and permeability on wellbore fracture pressure in the case of considering the seepage force.

2. Stresses around a Vertical Wellbore

2.1. Tradition Model. Conventionally, the stress analysis of a vertical wellbore at an interested depth during hydraulic fracturing is simplified as a plane problem [25, 26]. As shown in Figure 1, a well with a radius of r_a is drilled in a formation with in situ horizontal principal stresses $S11$ and $S22$ ($S11 > S22$). In a cylindrical coordinate system (r, θ), the stresses at any point are the radial stress σ_r and circumferential stress σ_θ, and tensile stresses were assumed to be negative in this paper. The circumferential stress S_θ^1 of the hollow square can be expressed as follows (all symbols in this paper are shown in Table 1):

$$S_\theta^1 = \frac{S11 + S22}{2}\left(1 + \frac{r_a^2}{r^2}\right) - \frac{S11 - S22}{2}\left(1 + \frac{3r_a^4}{r^4}\right)\cos 2\theta. \tag{1}$$

When the wellbore is pressurized by the injected fracturing fluid during hydraulic fracturing, two circumferential stresses S_θ^2 and S_θ^3 will be yielded at any point. The S_θ^2 is caused by the fluid pressure p_a at the borehole wall, which can be viewed as an internal pressure acting on a hollow thick cylinder.

$$S_\theta^2 = \frac{-p_a r_a^2}{r_e^2 - r_a^2} + \frac{-p_a r_a^2 r_e^2}{r^2(r_e^2 - r_a^2)}. \tag{2}$$

The third stress S_θ^3 is introduced by the pore pressure variation in the formation when the fracturing fluid penetrates into the formation and flows through its pores. When the formation pore pressure changes, the rock skeleton undergoes an uneven elastic deformation, causing so-called S_θ^3 stress under the mutual constraint of the skeleton elements [27–30]:

$$S_\theta^3 = A\left[\frac{1}{r^2}\frac{r^2 + r_a^2}{r_e^2 - r_a^2}\int_{r_a}^{r_e}(p(r) - p_o)rdr + \frac{1}{r^2}\int_{r_a}^{r}(p(r) - p_o)rdr - (p(r) - p_o)\right], \tag{3}$$

$$A = \frac{1 - 2\nu}{1 - \nu}\left(1 - \frac{K_B}{K_M}\right), \tag{4}$$

where $p(r)$ is the pore pressure distribution around the wellbore (Pa); p_o is the initial pore pressure (Pa); ν is Poisson's ratio, dimensionless; and K_B and K_M are the frame and matrix bulk moduli of the rock (Pa).

If the wellbore pressurization rate is relatively small and the fluid is noncompressible, the pore pressure distribution around the wellbore can be regarded as steady-state. This quasistatic pressure field in a domain with constant permeability is governed by the Laplace equation:

$$\frac{\partial^2 p}{\partial r^2} + \frac{1}{r}\frac{\partial p}{\partial r} = 0. \tag{5}$$

Once wellbore pressure p_a and pore pressure p_b at outer boundary r_e were determined, Equation (5) was solved by polar coordinates, and pore pressure distribution $p(r)$ around the wellbore during steady-state flow was obtained as follows [2, 31, 32]:

$$p(r) = p_a - (p_a - p_b)\frac{\ln r - \ln r_a}{\ln r_e - \ln r_a}. \tag{6}$$

By taking the pore pressure distribution $p(r)$ around the wellbore in Equation (6) into Equation (4), circumferential stress S_θ^3 due to pore pressure variation at any point under steady-state flow was obtained as ($r_e^2 \geq r_a^2$)

$$S_\theta^3 = \frac{A}{r^2}\left[\frac{r^2 - r_a^2}{2}(p_a - p_o) + \frac{p_a - p_b}{\ln(r_e/r_a)}\frac{r^2}{2}\ln\left(\frac{r_a}{r}\right) + \frac{r^2 - r_a^2}{4}\frac{p_a - p_b}{\ln(r_e/r_a)}\right] - A\left[p_a - p_o - (p_a - p_b)\frac{\ln(r/r_a)}{\ln(r_e/r_a)}\right]. \tag{7}$$

2.2. Introduction of Seepage Force

2.2.1. Mechanism of Seepage Force. As a viscous fluid flows through the pores of a porous media, the fluid imparts a friction force and normal thrust to the solid element of the matrix. The force is normally called seepage force in soil mechanics. Seepage force has long been considered in

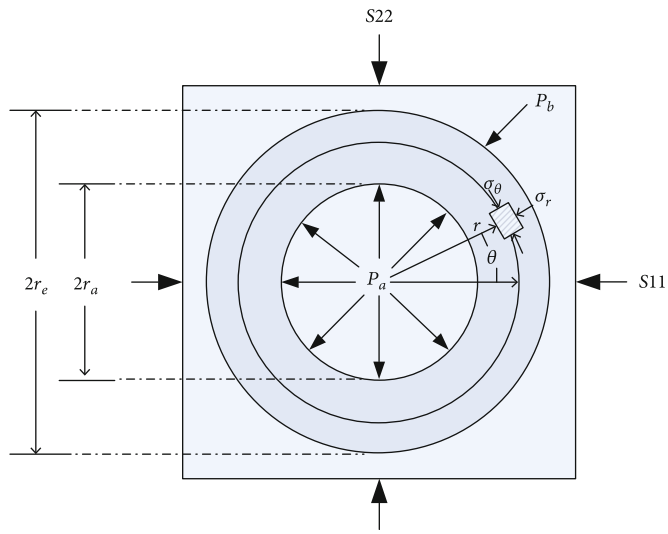

Figure 1: The cross-sectional graph of a vertical wellbore.

Table 1: Common symbols and units.

Symbol	The meaning of symbol	Unit
σ_r	Radial stress	Pa
σ_θ	Circumferential stress	Pa
$\tau_{r\theta}$	Shear stress	Pa
ν	Poisson's ratio	/
K_B	Frame bulk moduli of rock	Pa
K_M	Mineral matrix bulk moduli of rock	Pa
θ	Radian	rad
r	Radial distance	m
$S11$	Maximum horizontal principal stress	Pa
$S22$	Minimum horizontal principal stress	Pa
p_o	Initial pore pressure	Pa
p_a	Wellbore pressure	Pa
p_b	Pore pressure at the outer boundary	Pa
$p(r)$	Pore pressure distribution around wellbore	Pa
r_a	Wellbore inner diameter	m
F_{sp}	Seepage force	Pa
r_e	Outer diameter of wellbore	m
Δp	Differential pressure	Pa
σ_f	Tensile strength of a rock	Pa
$\sigma_\theta{}'$	The effective circumferential stress	Pa
S_θ^1	Circumferential total stress formed by formation principal stress	Pa
S_θ^2	Circumferential stress formed by wellbore pressure	Pa
S_θ^3	Circumferential stress formed by changes in pore pressure	Pa
S_θ^4	Circumferential stress formed by seepage force	Pa
K	Permeability	m^2
Q	Flow rate of fluid	m^3/s
μ	Fluid viscosity	Pa/s

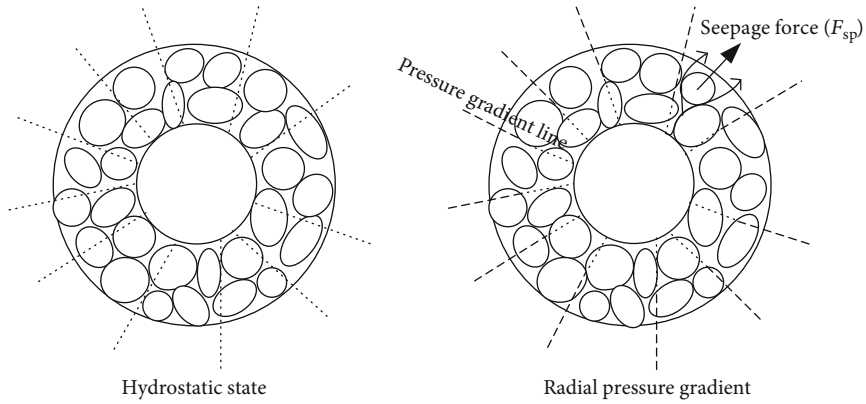

Figure 2: Schematic graph of a seepage force around a wellbore.

geotechnical engineering to assess the stability of a slope or the risk of sand liquefaction of dams [22, 33, 34] although its definition is still arguing in the engineering. In the paper, seepage force is defined as follows:

$$\vec{F}_{\text{sp}} = -\gamma_w i, \tag{8}$$

where i denotes pressure head gradient, dimensionless, and γ_w is the unit weight of fluid (N/m^3).

For the radial flow in Figure 1, the seepage force is simplified as follows:

$$F_{\text{sp}} = -\frac{\partial p(r)}{\partial r}. \tag{9}$$

The direction of the seepage force is in the opposite direction of the pressure gradient.

During hydraulic fracturing, high pressure wellbore fluid flows into rock and the in situ pore pressure changes. Pore fluid flowing zone around the wellbore with certain pore pressure gradient will be formed. As shown in Figure 2, rock matrix around a vertical wellbore satisfies the total stress equilibrium equation under stable state.

$$\begin{cases} \dfrac{\partial \sigma_r}{\partial r} + \dfrac{1}{r}\dfrac{\partial \tau_{r\theta}}{\partial \theta} + \dfrac{\sigma_r - \sigma_\theta}{r} - R = 0, \\ \dfrac{1}{r}\dfrac{\partial \sigma_\theta}{\partial \theta} + \dfrac{\partial \tau_{r\theta}}{\partial r} + \dfrac{2\tau_{r\theta}}{r} - S = 0, \end{cases} \tag{10}$$

where R is the radial volume force per unit volume and S is the circumferential volume force per unit volume. When the fluid flows radially, $R = F_{\text{sp}}$, $S = 0$. Under axisymmetric conditions, both the circumferential stress σ_θ and the radial stress σ_r are only functions of r, and the shear stress $\tau_{r\theta}$ is 0. Therefore, Equation (10) is reduced to

$$\frac{d\sigma_r}{dr} + \frac{\sigma_r - \sigma_\theta}{r} = F_{\text{sp}}. \tag{11}$$

As shown in Figure 2, when the fluid was under hydrostatic pressure state, pore pressure gradients in radius direction $\partial p/\partial r$ is equal to 0, and there is no seepage force. However, when fracturing fluid flows in the radial direction during hydraulic fracturing, there are pore pressure gradients $\partial p/\partial r$, and there is a seepage force F_{sp}. The direction of F_{sp} is consistent with the direction of fluid flowing.

2.2.2. Calculation of Seepage Force Stress Field. To study the effect of seepage force, solve the seepage force equation (Equation (11)). The internal and external boundary stresses are zero as the effects of wellbore pressure p_a and pore pressure p_b at outer boundary are already taken into account in Equation (11).

$$\begin{cases} \sigma_r = 0, & r = r_a, \\ \sigma_r = 0, & r = r_e. \end{cases} \tag{12}$$

Combining Equations (6), (11), and (12), the circumferential stress S_θ^4 formed by the seepage force under the plane strain condition during the steady-state flowing of wellbore fluid into a vertical wellbore:

$$S_\theta^4 = \frac{p_a - p_b}{2(1-\nu)}\left[\frac{\ln r - \ln r_a + 2\nu - 1}{\ln r_e - \ln r_a} - \frac{r_e^2\left(r^2 + {r_a}^2\right)}{r^2\left({r_e}^2 - {r_a}^2\right)}\right]. \tag{13}$$

It is well known that rock failure is controlled by the Terazaghi's effective stress [35]. The theory assumes when the effective circumferential stress $\sigma_\theta{}'$ reaches the tensile strength of a rock (σ_f), at borehole wall, tensile fracture at the wellbore occurs [2, 5, 12].

$$\sigma_\theta' \geq \sigma_f. \tag{14}$$

To compare with traditional methods, three cases are considered: rock is impermeable, pressured wellbore fluid flows into rock without considering seepage force effect, and pressured wellbore fluid flows into rock with seepage force effect.

When considering the rock is impermeable, the total effective circumferential stress is expressed as follows:

$$\sigma_\theta' = S_\theta^1 + S_\theta^2 - p_o. \tag{15}$$

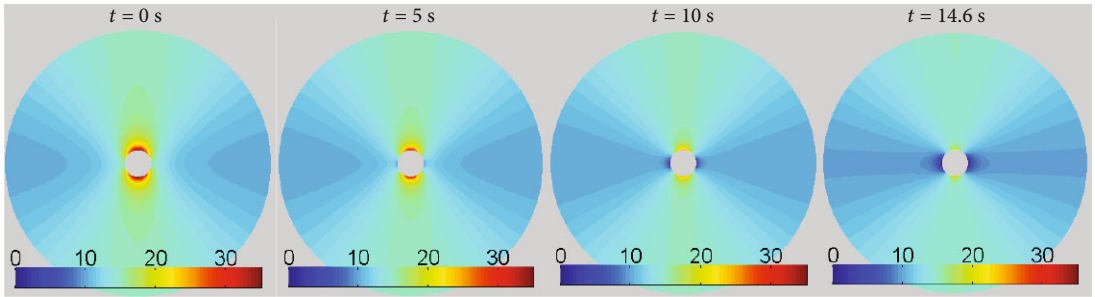

Figure 3: Wellbore breakdown process for impermeable rock case.

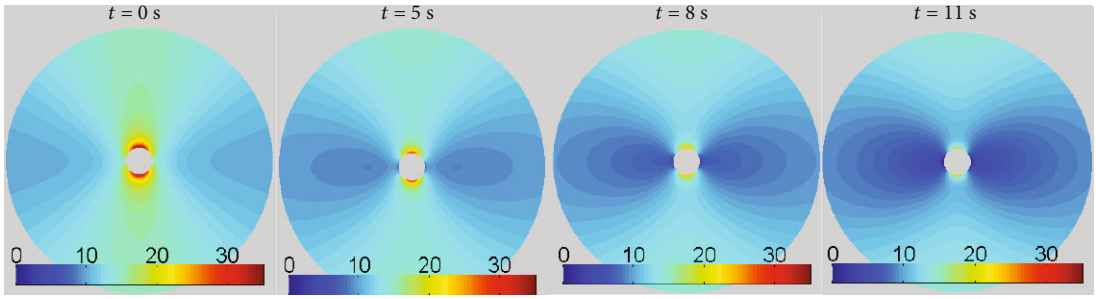

Figure 4: Wellbore breakdown process for the case of wellbore fluid flowing into rock but no seepage force.

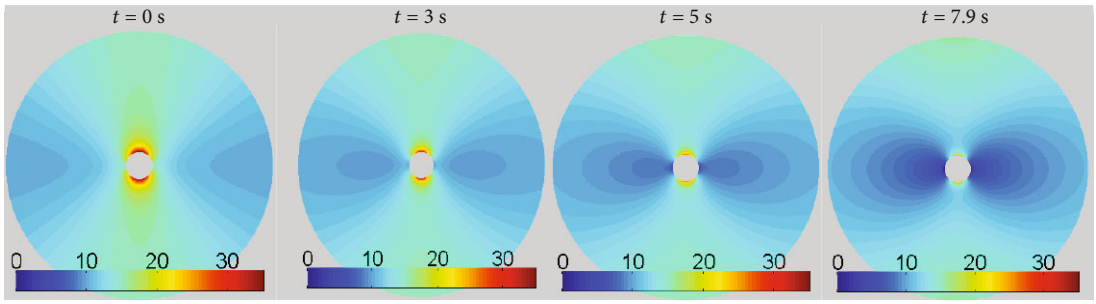

Figure 5: Wellbore breakdown process for the case of wellbore fluid flowing into rock and accounting seepage force.

When considering the fact that pressured wellbore fluid flows into the rock without considering seepage force effect,

$$\sigma'_\theta = S^1_\theta + S^2_\theta + S^3_\theta - p(r). \tag{16}$$

When considering the effect of seepage force (S^4_θ), the total effective circumferential stress is

$$\sigma'_\theta = S^1_\theta + S^3_\theta + S^4_\theta - p(r). \tag{17}$$

Note, in Equation (17), S^2_θ is not included as the effect of wellbore pressure (pa) is already considered in S^4_θ.

3. Analyses of Fracture Initiation under Seepage Force

3.1. Comparison of Wellbore Breakdown Process for Three Cases. In Section 2, circumferential stress fields around a wellbore wall and corresponding formation breakdown conditions are derived for steady-state fluid flow condition. During hydraulic fracturing operation, wellbore pressurization rates are relatively slow. The operation can be modeled using quasi-static conditions [2].

The calculation conditions are given as follows. Considering a vertical circular wellbore borehole drilled in an isotropic geologic medium, a 2D isotropic plane is used in the analysis (Figure 1). The maximum and minimum horizontal stresses are $S11 = 20$ MPa and $S22 = 15$ MPa. The initial wellbore pressure p_a and pore pressure p_o is assumed as 5 MPa. The tensile strength of the rock σ_f is taken as 0 MPa. The Poisson's ratio in the isotropic plane is 0.25. The inner and outer diameters of the wellbore are supposed as 1 dm and 10 dm, respectively. It is assumed that starting from $t = 0$ s, the wellbore pressure starts to increase at a rate of 1 MPa/s until the wellbore wall is broken. That is, the effective circumferential stress $\sigma_\theta{}'$ reaches the tensile strength of the rock σ_f.

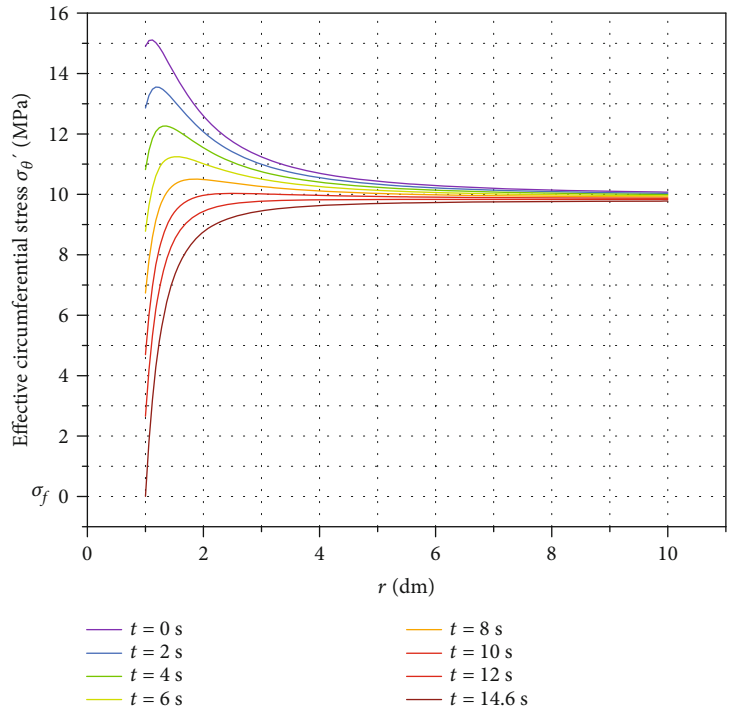

Figure 6: The variation of σ_θ' with radial distance for impermeable rock.

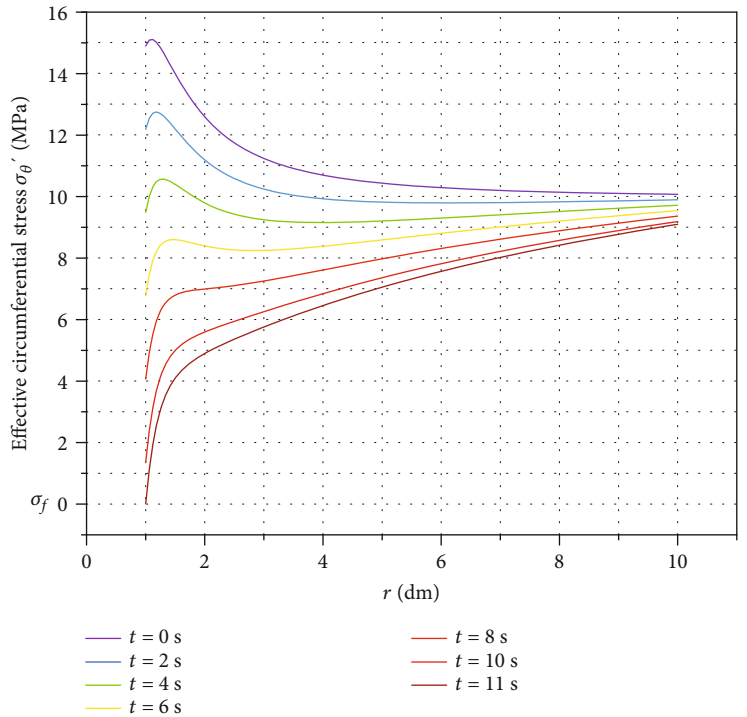

Figure 7: The variation of σ_θ' with radial distance for the case of wellbore fluid flowing into rock but no seepage force.

The pore pressure at the outer boundary of wellbore during the entire pressurization process is maintained at p_o ($p_b = p_o$).

Equations (15)–(17) represent the three cases: rock is impermeable, pressured wellbore fluid flows into rock without considering seepage force effect, and pressured wellbore fluid flows into rock with seepage force effect. Using the given conditions, the wellbore breakdown processes for the three cases are calculated under quasistatic conditions.

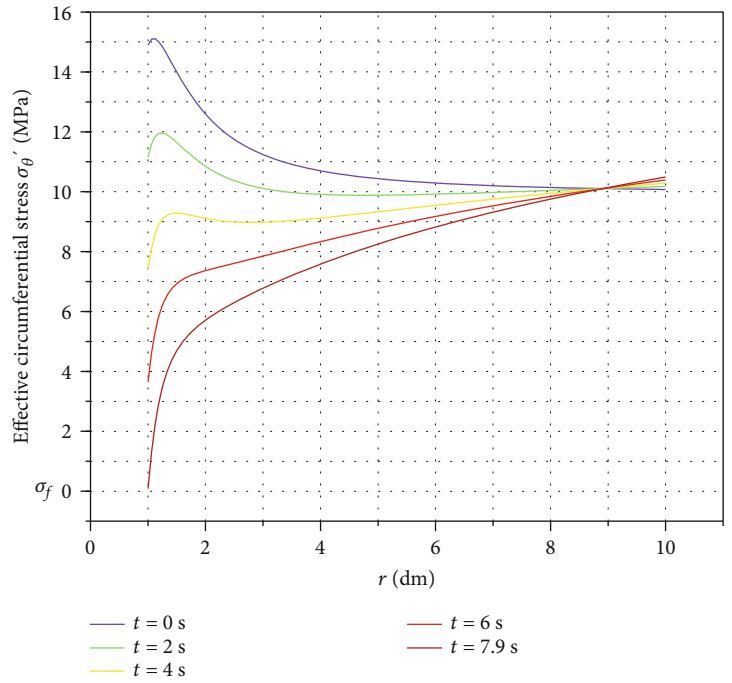

Figure 8: The variation of σ_θ' with radial distance for the case of wellbore fluid flowing into rock and accounting seepage force.

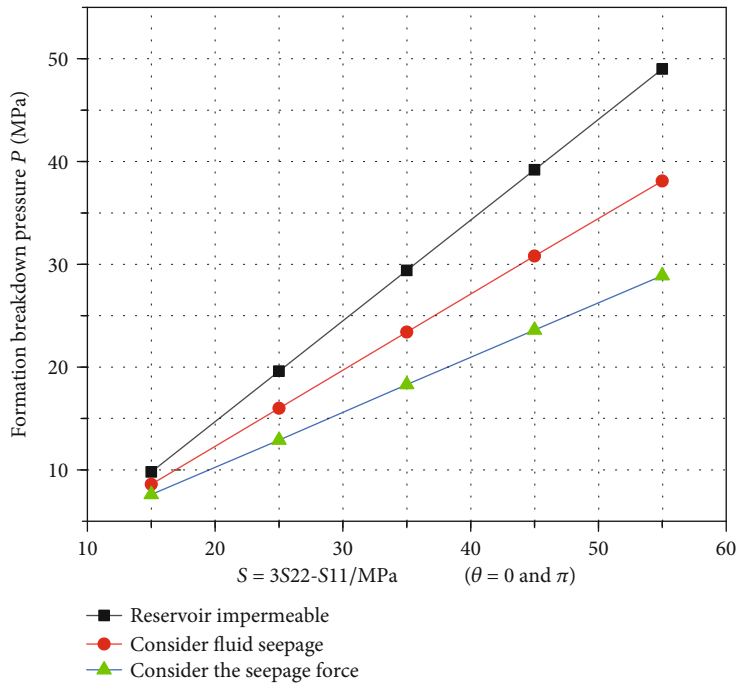

Figure 9: Formation breakdown pressures from the three cases when $S11$ and $S22$ increase uniformly.

The calculated results for the three cases are shown in Figures 3–5 (color ruler scale corresponds to the effective circumferential stress value σ_θ').

From Figures 3–5, at time $t = 0$ s, the wellbore has not been pressurized, and there is apparent stress concentration at the wellbore wall. As the wellbore is pressurized, the effective circumferential compressive stress σ_θ' around the wellbore gradually decreases and the stress concentration gradually disappears. The breakdown points at the wellbore wall for the three cases are in the directions of maximum horizontal principal stress $S11$ ($\theta = 0$ and π). When fluid flows into the formation (Figure 4), the stress field varies

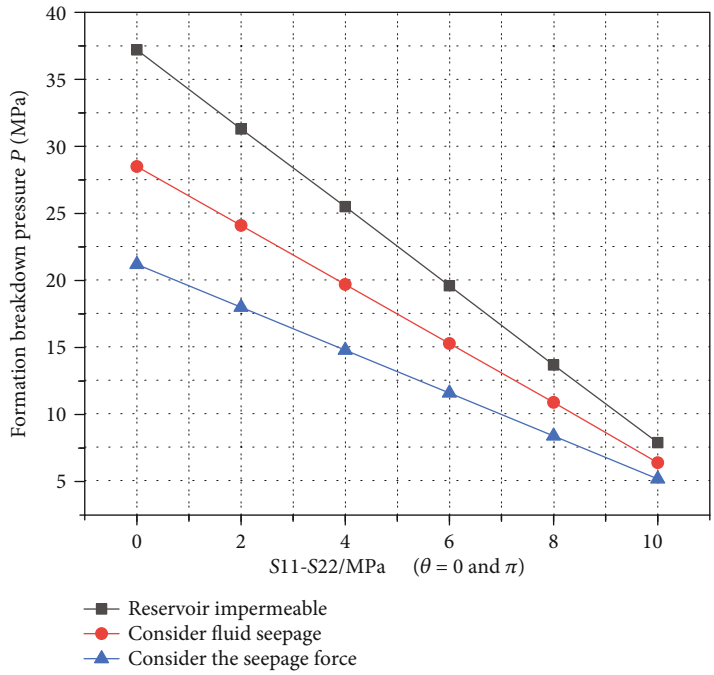

Figure 10: Formation breakdown pressures from the three cases when the difference between $S11$ and $S22$ varies.

more intensely comparing to Case 1 (Figure 3). This proves that fluid flowing into wellbore process should be considered during the analysis of hydraulic fracturing. Under the action of seepage force, as shown in Figure 5, the wellbore wall will be broken very quick, taking only 7.9 s. The effect of seepage force is markedly conducive to wellbore breakdown.

Figures 6–8 show the variations of the effective circumferential stresses $\sigma_\theta{}'$ along the direction of the maximum horizontal principal stress $S11$ for the three cases. From Figures 6–8, the effective circumferential stress $\sigma_\theta{}'$ from the wellbore wall r_a decreases the fastest, and the decreasing speed becomes slower gradually as r increases. For impermeable rock (Case 1), $\sigma_\theta{}'$ trends to no variation anymore from the distance of $r = 6.5r_a$ (Figure 6). When fluid flows in the wellbore, due to the variation of the pore pressure $p(r)$, $\sigma_\theta{}'$ varies in the whole modeling area. For the effect of seepage force (Case 3), the effective circumferential compressive stress $\sigma_\theta{}'$ around the outer boundary even exceeds the initial stress state, indicating that the seepage force gives a compression effect at the outer boundary at the case condition (Figure 8).

3.2. Wellbore Breakdown Pressure under Different Outer Boundary Conditions. To study the effect of formation in situ stresses on wellbore breakdown for the three cases, two situations of varying formation maximum and minimum horizontal principal stresses are given. One situation is $S11$ and $S22$ increasing uniformly while keeping the difference between $S11$ and $S22$ unchanged. The other situation is that the difference between $S11$ and $S22$ is different.

From Equation (1), the circumferential compressive stress generated by $S11$ and $S22$ at the well wall in the direction of maximum stress $S22$ ($\theta = 0$ or π) is $S(S = 3S22\text{-}S11)$. When $S11$ and $S22$ increase uniformly, S indicates the change in the stress concentration of the well wall and the magnitude of the compressive stress value that needs to be overcome to breakdown the wellbore wall by the fluid pressure in the wellbore. Figure 9 shows the calculated breakdown pressure versus the S values as $S11$ and $S22$ increase uniformly. From Figure 9, when $S11$ and $S22$ increase uniformly, the formation breakdown pressure increases linearly for the three cases. With S increasing, the gap of the formation breakdown pressure values for the seepage force case (Case 3) is getting greater for other two cases. The effect of seepage force becomes more and more significant as the principal stresses of the formation increase uniformly.

Figure 10 gives the variation of formation breakdown pressure with the difference of the two in situ stresses ($S11$ -$S22$). From Figure 10, for the three cases, with the increasing of $S11$-$S22$, formation breakdown pressure decreases linearly and the gap of the formation breakdown pressure values for seepage force case and the other cases is getting smaller. The higher the difference between $S11$ and $S22$, the smaller the effect of the seepage force.

4. Effect of Seepage Force for Different Permeability Rock

Steady-state fluid flow in porous media is controlled by Darcy's law. For given fluid pressure in a wellbore and pore pressure, the smaller the rock permeability, the greater the pressure difference Δp in wellbore radial direction. Therefore, the effect of seepage force on formation breakdown pressure will be affected by the rock permeability.

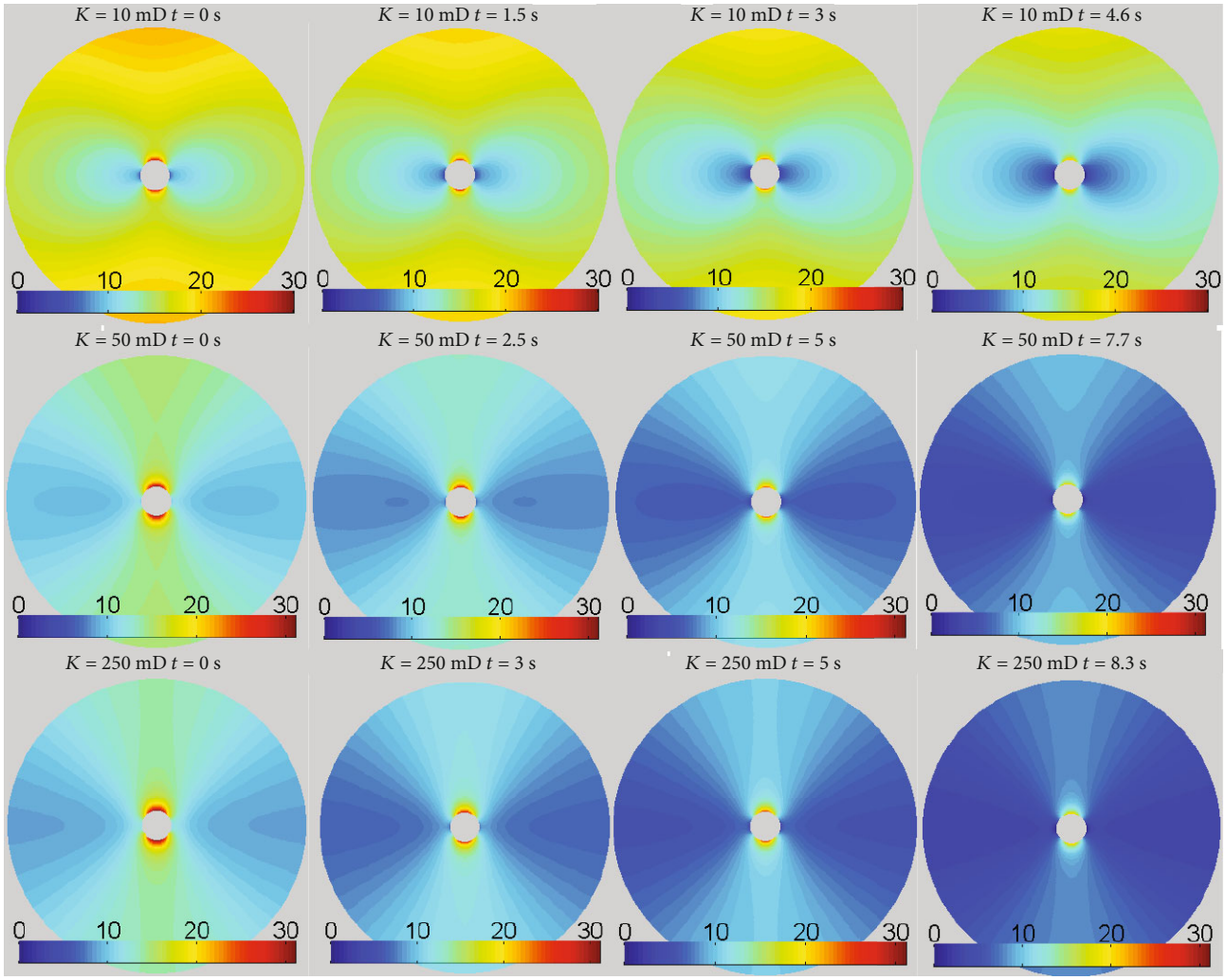

Figure 11: Formation breakdown process for three permeability rocks accounting seepage force.

Using the same condition in Section 3.1, the formation breakdown pressures are analysed with various permeabilities for the three cases. Noting that in this section the pore pressure p_b at the outer boundary r_e is determined by the rock permeability K ($Q = 0.1\ \text{cm}^3/\text{s}$; $L = 10\ \text{dm}$; $\mu = 1\ \text{mPa·s}$). During wellbore pressurization, different stable differential pressures Δp are formed around the wellbore with different permeability ($K = 10\ \text{mD}$, $\Delta p = 10\ \text{MPa}$; $K = 50\ \text{mD}$, $\Delta p = 2\ \text{MPa}$; $K = 250\ \text{mD}$, $\Delta p = 0.4\ \text{MPa}$).

The formation breakdown process of the three different permeability rocks under the acting of seepage force is shown in Figure 11.

As shown in Figure 11, low-permeability rock ($K = 10\ \text{mD}$) is the first to initiate fracture under the action of seepage forces due to higher pressure differences and pore pressure gradients. As the pore pressure gradient is small and the effect of seepage force is not significant, the fracture initiation of high permeability rock ($K = 250\ \text{mD}$) is slowest to get breakdown pressure. Although the pressure difference between the inner and outer boundaries of the high-permeability reservoir is small, the pore pressure at each point $p(r)$ is relatively great. Therefore, the area where the effective circumferential stress field around the wellbore of the high-permeability reservoir is disturbed during which wellbore pressurization is more significant than that of the low-permeability rock.

In addition, the relationships between formation breakdown pressure and permeability for the three cases are shown in Figure 12. Figure 13 gives the ratio between the formation breakdown pressure of the case with seepage force and those from other two cases.

It can be seen from Figures 12 and 13 that the formation breakdown pressure for the case of fluid flowing into rock is smaller than that for impermeable rock. As the permeability increases, the effect of seepage force becomes less important, and the formation breakdown pressure is gradually approaching that without considering the effect of seepage force.

The effect of seepage force is more significant in low-permeability rock, where the formation breakdown pressure is only 20.65% of the breakdown pressure of ignoring seepage force. Therefore, the effect of seepage force should be applied during the analysis of hydraulic fracturing.

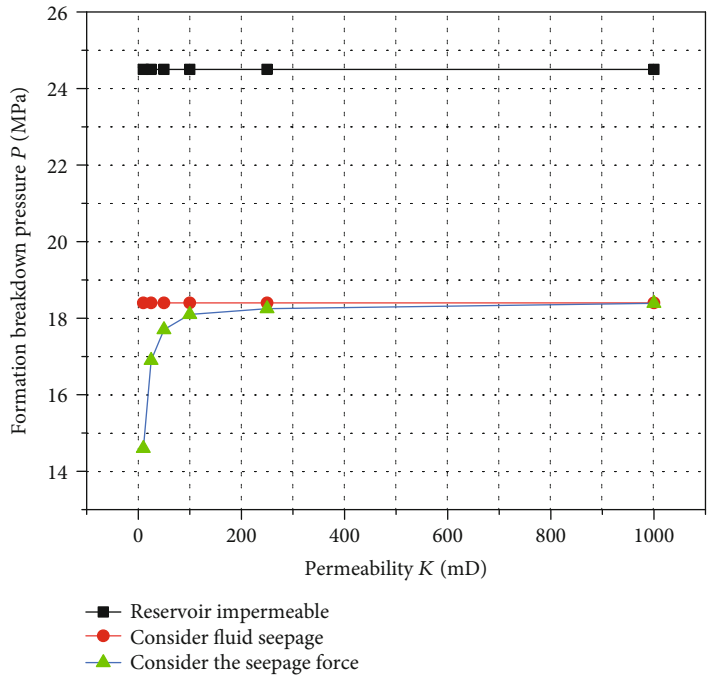

Figure 12: Relationship between formation breakdown pressure and permeability for three cases.

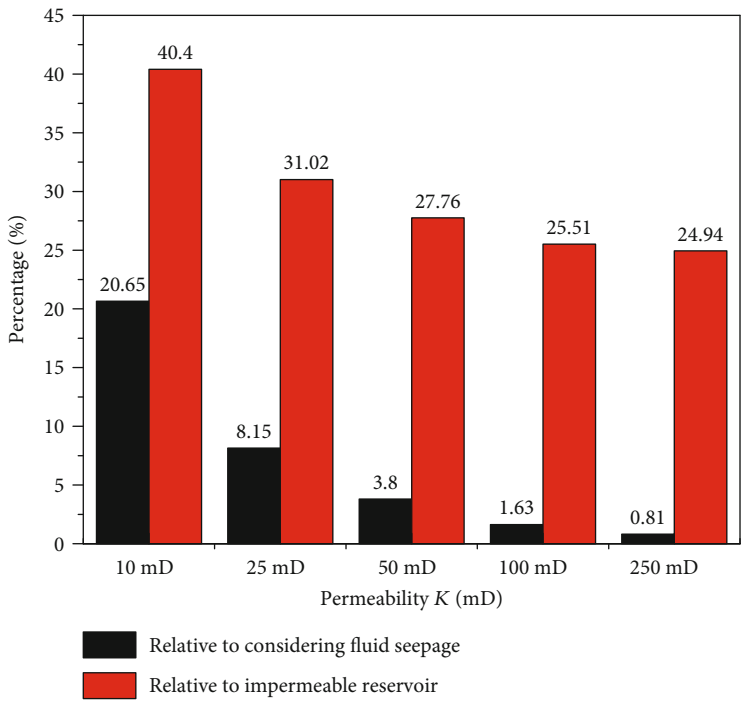

Figure 13: Reduction percentage of formation breakdown pressure from the case of considering seepage force to those from other cases.

5. Conclusions

(1) During hydraulic fracturing, wellbore fluid flows into wellbore and will yield a seepage force due to fluid drag forces. The seepage force acts on the rock matrix in the fluid flowing direction and could be measured by pore pressure gradient

(2) For a vertical well, the seepage force is beneficial to breakdown the formation and thus lowers the wellbore breakdown pressure

(3) The effect of seepage force on formation breakdown increases as the two horizontal principal stresses increase uniformly. Therefore, the deeper a formation, the greater action of the seepage force

(4) The greater the difference of the two horizontal principal stresses, the lower effect of seepage force on formation breakdown. Therefore, seepage force gives more contribution to breakdown formation for isotropy formation or formations with small difference of the two horizontal stresses such as unconventional reservoirs

(5) The greater the pore pressure gradient, the greater the seepage force. Seepage force increases as rock permeability decreases, and it should not be ignored in hydraulic fracturing analysis, especially for low-permeability formation

Data Availability

The [DATA TYPE] data used to support the findings of this study are available from the corresponding author upon request at deshengzhou@126.com.

Conflicts of Interest

The authors declare no conflict of interest.

Acknowledgments

This work was supported by the National Natural Science Foundation of China (Grant Nos. 51934005, 51874242, and 51904244); the National Science and Technology Major Project of China (Grant No. 2016ZX05050-009); the Natural Science Basic Research Plan in Shaanxi Province of China (Program No. 2019JQ-364); and the Scientific Research Program Funded by Shaanxi Provincial Education Department (Program No. 19JK0663).

References

[1] B. Haimson and C. Fairhurst, "Initiation and extension of hydraulic fractures in rocks," *Society of Petroleum Engineers Journal*, vol. 7, no. 3, pp. 310–318, 1967.

[2] B. Haimson, *Hydraulic Fracturing in Porous and Nonporous Rock and its Potential for Determining In-Situ Stresses at Great Depth*, 1968.

[3] B. Haimson and C. Fairhurst, "Hydraulic fracturing in porous-permeable materials," *Journal of Petroleum Technology*, vol. 21, no. 7, pp. 811–817, 1969.

[4] B. Haimson and C. Fairhurst, "In-situ stress determination at great depth by means of hydraulic fracturing," in *The 11th US Symposium on Rock Mechanics (USRMS). American Rock Mechanics Association*, Berkeley, CA, USA, June 1969.

[5] M. K. Hubbert and D. G. Willis, *Mechanics of Hydraulic Fracturing*, 1972.

[6] W. L. Medlin and L. Masse, "Laboratory investigation of fracture initiation pressure and orientation," *Society of Petroleum Engineers Journal*, vol. 19, no. 2, pp. 129–144, 1979.

[7] F. Guo, N. R. Morgenstern, and J. D. Scott, "Interpretation of hydraulic fracturing breakdown pressure," *International Journal of Rock Mechanics and Mining Sciences & Geomechanics Abstracts. Pergamon*, vol. 30, no. 6, pp. 617–626, 1993.

[8] I. Song, M. Suh, K. S. Won, and B. Haimson, "A laboratory study of hydraulic fracturing breakdown pressure in tablerock sandstone," *Geosciences Journal*, vol. 5, no. 3, pp. 263–271, 2001.

[9] A. P. Bunger, A. Lakirouhani, and E. Detournay, "Modelling the effect of injection system compressibility and viscous fluid flow on hydraulic fracture breakdown pressure," in *Rock stress and earthquakes-proceedings of the 5th international symposium on in-situ rock stress*, pp. 59–67, Beijing, China, August 2010.

[10] S. J. Ha, J. Choo, T. S. Yun, and C. O. Liquid, "Liquid CO2 fracturing: effect of fluid permeation on the breakdown pressure and cracking behavior," *Rock Mechanics and Rock Engineering*, vol. 51, no. 11, pp. 3407–3420, 2018.

[11] Z. Tariq, M. Mahmoud, A. Abdulraheem, A. al-Nakhli, and M. BaTaweel, "An experimental study to reduce the breakdown pressure of the unconventional carbonate rock by cyclic injection of thermochemical fluids," *Journal of Petroleum Science and Engineering*, vol. 187, p. 106859, 2020.

[12] T. Ito and K. Hayashi, "Physical background to the breakdown pressure in hydraulic fracturing tectonic stress measurements," *International Journal of Rock Mechanics and Mining Sciences & Geomechanics Abstracts. Pergamon*, vol. 28, no. 4, pp. 285–293, 1991.

[13] T. Ito, "Effect of pore pressure gradient on fracture initiation in fluid saturated porous media: Rock," *Engineering Fracture Mechanics*, vol. 75, no. 7, pp. 1753–1762, 2008.

[14] X. Jin, S. N. Shah, J. C. Roegiers et al., "Breakdown pressure determination-a fracture mechanics approach," in *SPE Annual Technical Conference and Exhibition. Society of Petroleum Engineers*, New Orleans, LA, USA, September 2013.

[15] H. Fatahi, M. M. Hossain, S. H. Fallahzadeh, and M. Mostofi, "Numerical simulation for the determination of hydraulic fracture initiation and breakdown pressure using distinct element method," *Journal of Natural Gas Science and Engineering*, vol. 33, pp. 1219–1232, 2016.

[16] C. Xiao, H. Ni, X. Shi, and R. Wang, "A fracture initiation model for carbon dioxide fracturing considering the bottom hole pressure and temperature condition," *Journal of Petroleum Science and Engineering*, vol. 184, p. 106541, 2020.

[17] R. Mourgues and P. R. Cobbold, "Some tectonic consequences of fluid overpressures and seepage forces as demonstrated by sandbox modelling," *Tectonophysics*, vol. 376, no. 1-2, pp. 75–97, 2003.

[18] P. R. Cobbold, B. J. Clarke, and H. Løseth, "Structural consequences of fluid overpressure and seepage forces in the outer

thrust belt of the Niger Delta," *Petroleum Geoscience*, vol. 15, no. 1, pp. 3–15, 2009.

[19] A. Zanella and P. R. Cobbold, *'Beef': Evidence for Fluid Overpressure and Hydraulic Fracturing in Source Rocks during Hydrocarbon Generation and Tectonic Events: Field Studies and Physical Modelling*, 2012.

[20] A. Rozhko, *Role of Seepage Forces on Hydraulic Fracturing and Failure Patterns*, 2007.

[21] A. Y. Rozhko, Y. Y. Podladchikov, and F. Renard, "Failure patterns caused by localized rise in pore-fluid overpressure and effective strength of rocks," *Geophysical Research Letters*, vol. 34, no. 22, 2007.

[22] C. Zhou, W. Shao, and C. J. van Westen, "Comparing two methods to estimate lateral force acting on stabilizing piles for a landslide in the Three Gorges Reservoir, China," *Engineering Geology*, vol. 173, pp. 41–53, 2014.

[23] J. Zou, S. Li, Y. Xu, H. C. Dan, and L. H. Zhao, "Theoretical solutions for a circular opening in an elastic–brittle–plastic rock mass incorporating the out-of-plane stress and seepage force," *KSCE Journal of Civil Engineering*, vol. 20, no. 2, pp. 687–701, 2016.

[24] H. AlKhafaji, M. Imani, and A. Fahimifar, "Ultimate bearing capacity of rock mass foundations subjected to seepage forces using modified Hoek–Brown criterion," *Rock Mechanics and Rock Engineering*, vol. 53, no. 1, pp. 251–268, 2020.

[25] M. D. Zoback, D. Moos, L. Mastin, and R. N. Anderson, "Well bore breakouts and in situ stress," *Journal of Geophysical Research: Solid Earth*, vol. 90, no. B7, pp. 5523–5530, 1985.

[26] A. J. Miles and A. D. Topping, "Stresses around a deep well," *Transactions of the AIME*, vol. 179, no. 1, pp. 186–191, 1949.

[27] W. Nowacki, *Thermoelasticity*, Elsevier, 2013.

[28] S. P. Timošenko and J. N. Goodier, *Theory of elasticity*, McGraw-Hill, 1951.

[29] J. R. Rice and M. P. Cleary, "Some basic stress diffusion solutions for fluid-saturated elastic porous media with compressible constituents," *Reviews of Geophysics*, vol. 14, no. 2, pp. 227–241, 1976.

[30] M. A. Biot, "General theory of three-dimensional consolidation," *Journal of Applied Physics*, vol. 12, no. 2, pp. 155–164, 1941.

[31] A. Y. Rozhko, "Benchmark for poroelastic and thermoelastic numerical codes," *Physics of the Earth and Planetary Interiors*, vol. 171, no. 1-4, pp. 170–176, 2008.

[32] J. Geertsma, "Problems of rock mechanics in petroleum production engineering," in *1st ISRM Congress. International Society for Rock Mechanics and Rock Engineering*, Lisbon, Portugal, September 1966.

[33] B. D. Collins and D. Znidarcic, "Stability analyses of rainfall induced landslides," *Journal of Geotechnical and Geoenvironmental Engineering*, vol. 130, no. 4, pp. 362–372, 2004.

[34] R. F. Craig, *Soil Mechanics*, ELBS Edition, Great Britain, 4th edition, 1987.

[35] K. Terazaghi, *Theoretical Soil Mechanics*, John Wiley and Sons, 1965.